Science Advances
AAAS

Supplementary Materials for

Reticular thalamic hyperexcitability drives autism spectrum disorder behaviors in the Cntnap2 model of autism

Sung-Soo Jang *et al.*

Corresponding author: John R. Huguenard, john.huguenard@stanford.edu

Sci. Adv. **11**, eadw4682 (2025)
DOI: 10.1126/sciadv.adw4682

The PDF file includes:

Figs. S1 to S8
Legends for movies S1 to S8

Other Supplementary Material for this manuscript includes the following:

Movies S1 to S8

Supplementary Figures

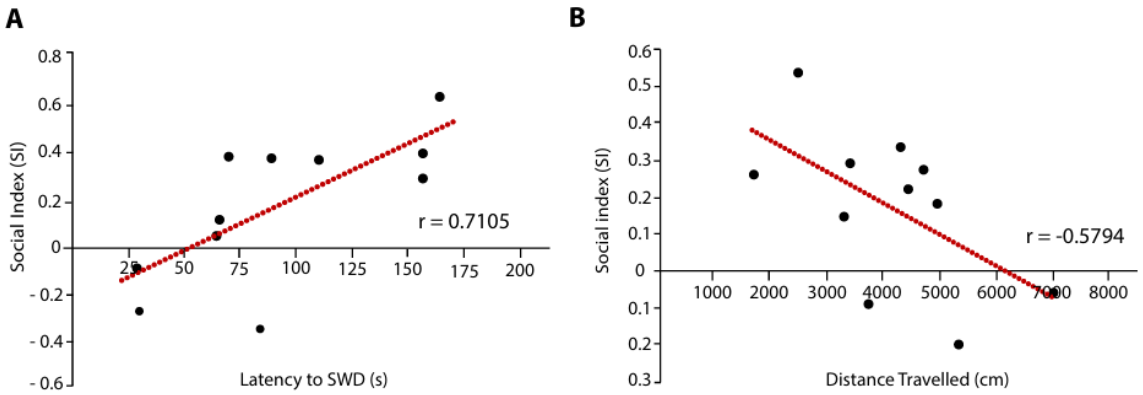

Fig. S1. Correlations between seizure propensity, locomotor activity, and social preference. (A-B) Scatter plots showing individual data points and linear regression analysis. **(A)** A positive correlation between latency to SWD and social index. **(B)** A negative correlation between total distance travelled and social index. Each dot represents an individual mouse. Red dashed lines indicate linear regression fits. Pearson's correlation coefficient (r) is indicated in each panel. (A-B) n = 11.

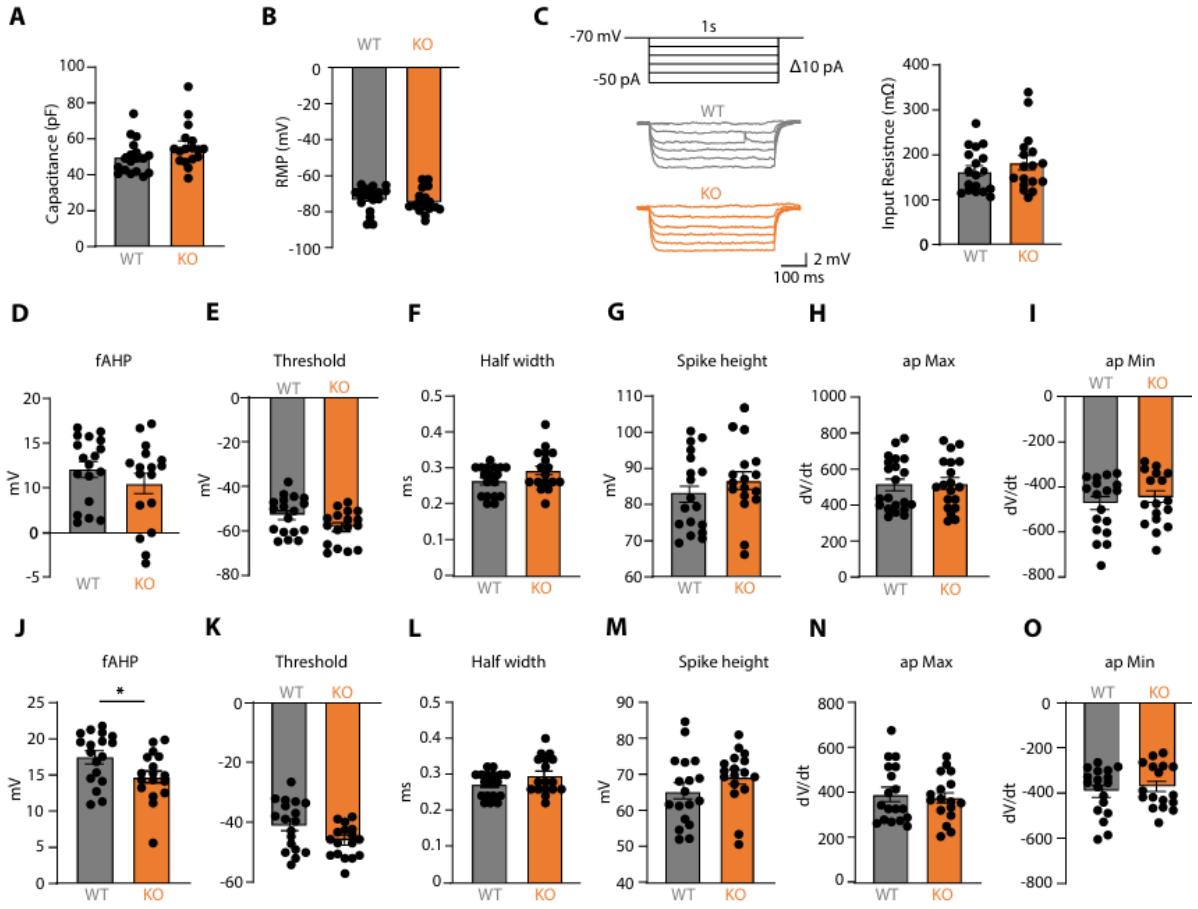

Fig. S2. Passive properties and AP properties in RT of *Cntnap2*$^{+/+}$ and *Cntnap2*$^{-/-}$ mice. (A-B) Quantification of membrane capacitance (A) and RMP (B) in RT of *Cntnap2*$^{+/+}$ and *Cntnap2*$^{-/-}$ mice. **(C)** Protocol and representative traces (left) showing voltage deflections elicited by –50 pA to 0 pA intracellular current injections and quantification (right) of input resistance (MΩ) from RT of *Cntnap2*$^{+/+}$ and *Cntnap2*$^{-/-}$ mice. **(D-I)** Quantification of AP properties, including fAHP (D), AP threshold (E), half width (F), spike height (G), ap max dV/dt (H), and ap min dV/dt (I) from 1st spike from RT of *Cntnap2*$^{+/+}$ and *Cntnap2*$^{-/-}$ mice. **(J-O)** Quantification of AP properties, including fAHP (J), AP threshold (K), half width (L), spike height (M), ap max dV/dt (N), and ap min dV/dt (O) from last spike from RT of *Cntnap2*$^{+/+}$ and *Cntnap2*$^{-/-}$ mice. (A-O) n = 18 for *Cntnap2*$^{+/+}$ and n =17 for *Cntnap2*$^{-/-}$. The statistical tests involved an unpaired two-tailed t-test (A-O). Data are represented as mean values ± SEM. *$P < 0.05$.

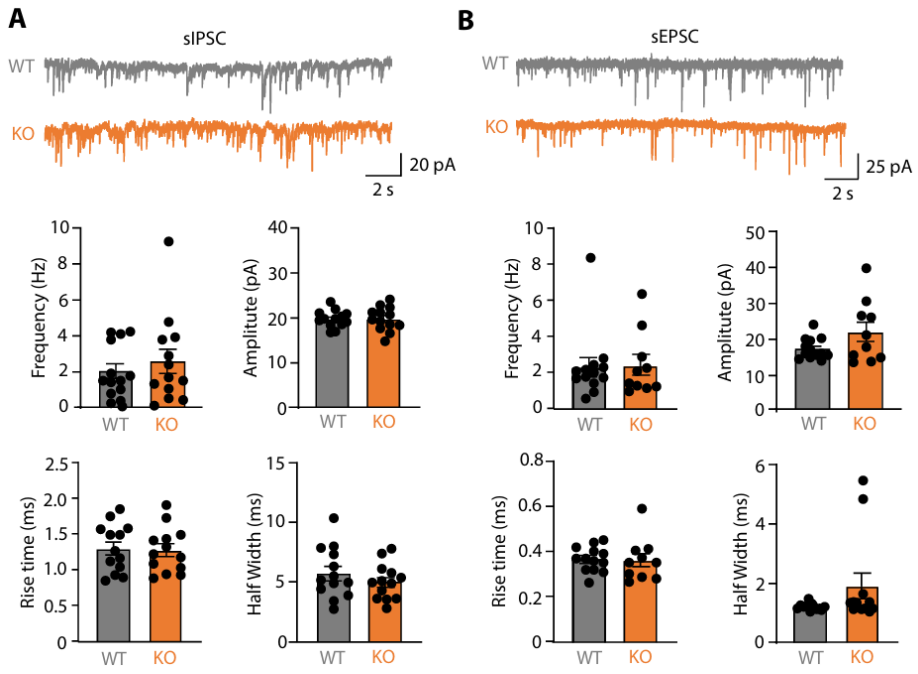

Fig. S3. sIPSCs and sEPSCs in RT of *Cntnap2*$^{+/+}$ and *Cntnap2*$^{-/-}$ mice. (A) Representative traces (top) showing spontaneous IPSCs and quantification (bottom) of sIPSC frequency (Hz), amplitude (pA), rise time (ms), and half-width (ms) from RT of *Cntnap2*$^{+/+}$ and *Cntnap2*$^{-/-}$ mice. (n = 13 for *Cntnap2*$^{+/+}$ and n = 13 for *Cntnap2*$^{-/-}$). **(B)** Representative traces (top) showing spontaneous EPSCs and quantification (bottom) of sEPSC frequency (Hz), amplitude (pA), rise time (ms), and half-width (ms) from RT of *Cntnap2*$^{+/+}$ and *Cntnap2*$^{-/-}$ mice. (n = 13 for *Cntnap2*$^{+/+}$ and n =10 for *Cntnap2*$^{-/-}$). The statistical tests involved an unpaired two-tailed t-test (A, B). Data are represented as mean values ± SEM.

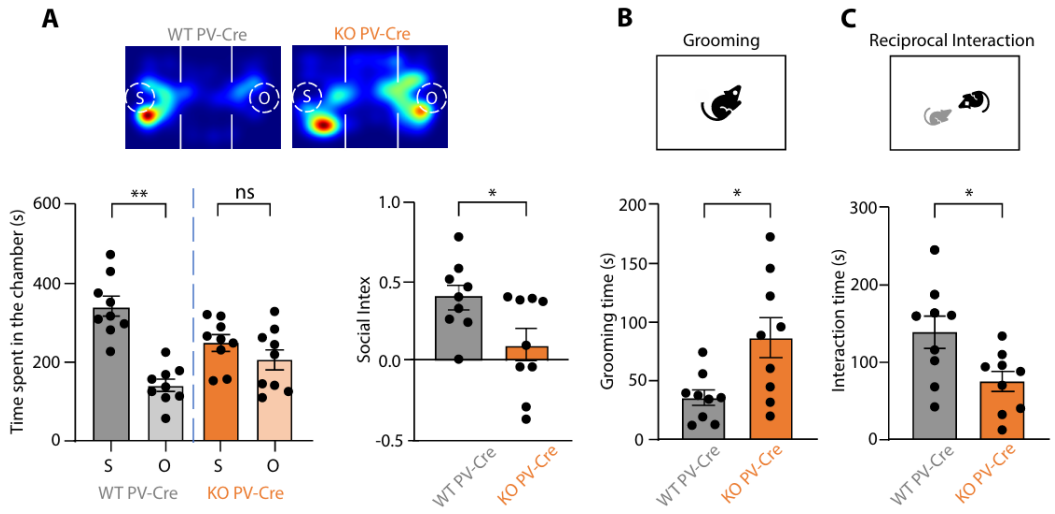

Fig. S4. Confirmation of deficits in ASD-related behaviors in *Cntnap2*$^{+/+}$ and *Cntnap2*$^{-/-}$ PV-Cre mice. (A) Representative heatmaps (top) showing location in social preference tests and quantification (bottom) of time spent in the chamber and social index, in *Cntnap2*$^{+/+}$ and *Cntnap2*$^{-/-}$ PV-Cre mice. **(B)** Quantification of grooming time in *Cntnap2*$^{+/+}$ and *Cntnap2*$^{-/-}$ PV-Cre mice. **(C)** Quantification of interaction time in *Cntnap2*$^{+/+}$ and *Cntnap2*$^{-/-}$ PV-Cre mice. (A-C) n = 9 for *Cntnap2*$^{+/+}$ PV-Cre and n = 9 for *Cntnap2*$^{-/-}$ PV-Cre. The statistical tests involved a paired two-tailed t-test (A) and an unpaired two-tailed t-test (A-C). Data are represented as mean values ± SEM. *P*-values in figure panels: **P* < 0.05; ***P* < 0.01.

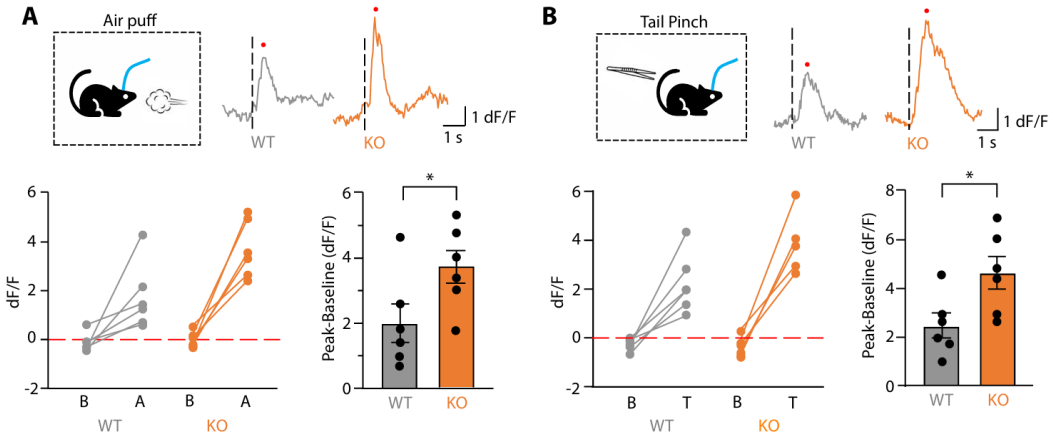

Fig. S5. Ca^{2+} response to external stimuli in *Cntnap2*$^{+/+}$ and *Cntnap2*$^{-/-}$ mice. (A) Schematic (top, left) illustrating the air puff, representative Ca^{2+} signal (top, right), and quantification (bottom) of peak dF/F and change in dF/F (bottom) during baseline and air puff in *Cntnap2*$^{+/+}$ and *Cntnap2*$^{-/-}$ mice. **(B)** Schematic (top, left) illustrating the tail pinch, representative Ca^{2+} signal (top, right), and quantification (bottom) of peak dF/F and change in dF/F during baseline and tail pinch in *Cntnap2*$^{+/+}$ and *Cntnap2*$^{-/-}$ mice. (A-B) n = 6 for *Cntnap2*$^{+/+}$ and n = 6 for *Cntnap2*$^{-/-}$. Red dot indicates peak. The statistical tests involved an unpaired two-tailed t-test (A-B). Data are represented as mean values ± SEM. *P*-values in figure panels: $*P < 0.05$.

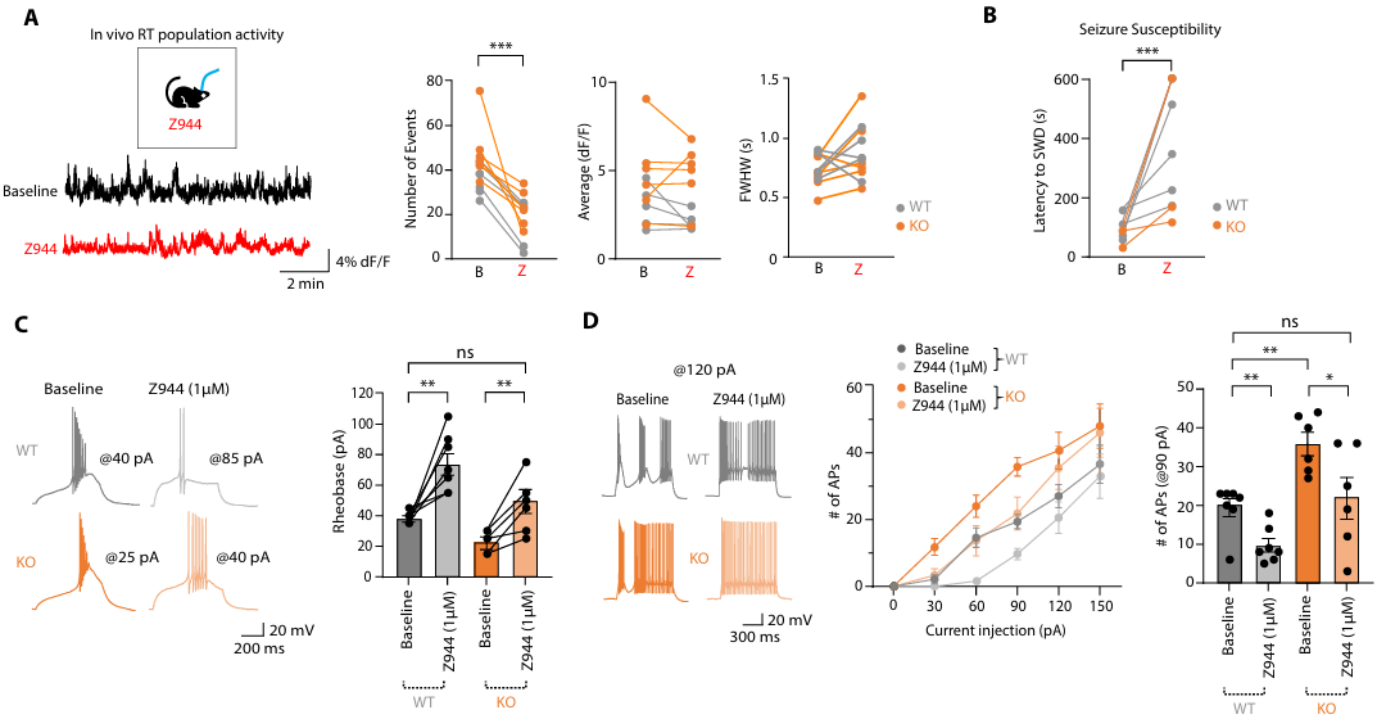

Fig. S6. Z944 suppresses in vivo RT population activity, increases latency to SWD in both *Cntnap2*$^{+/+}$ and *Cntnap2*$^{-/-}$ mice, and restores rheobase and intrinsic excitability in *Cntnap2*$^{-/-}$ mice. (A) Schematic (left, top) illustrating experimental strategy, representative fiber photometry signals (left, bottom) of spontaneous Ca^{2+} fluctuations, and quantification (right) of the number of events, average dF/F, and FWHM of Ca^{2+} dynamics during baseline and Z944 condition. (n = 5 for *Cntnap2*$^{+/+}$ and n = 6 for *Cntnap2*$^{-/-}$). **(B)** Quantification of latency to SWD during baseline and Z944 condition. **(C)** Representative traces (left) showing initial burst firing elicited by rheobase currents and quantification (right) of rheobase currents (pA) during baseline and 1 µM Z944. **(D)** Representative traces (left) showing APs elicited by 120 pA, quantification (middle) of the number of evoked APs elicited by 0 – 150 pA, and quantification (right) of the number of APs elicited by 90 pA injection during baseline and Z944. (C-D) n = 7 for *Cntnap2*$^{+/+}$ and n = 6 for *Cntnap2*$^{-/-}$. The statistical tests involved a paired two-tailed t-test (A-D) and two-way ANOVA with Tukey's test (C-D). Data are represented as mean values ± SEM. *P*-values in figure panels: **P* < 0.05; ***P* < 0.01; ****P* < 0.001.

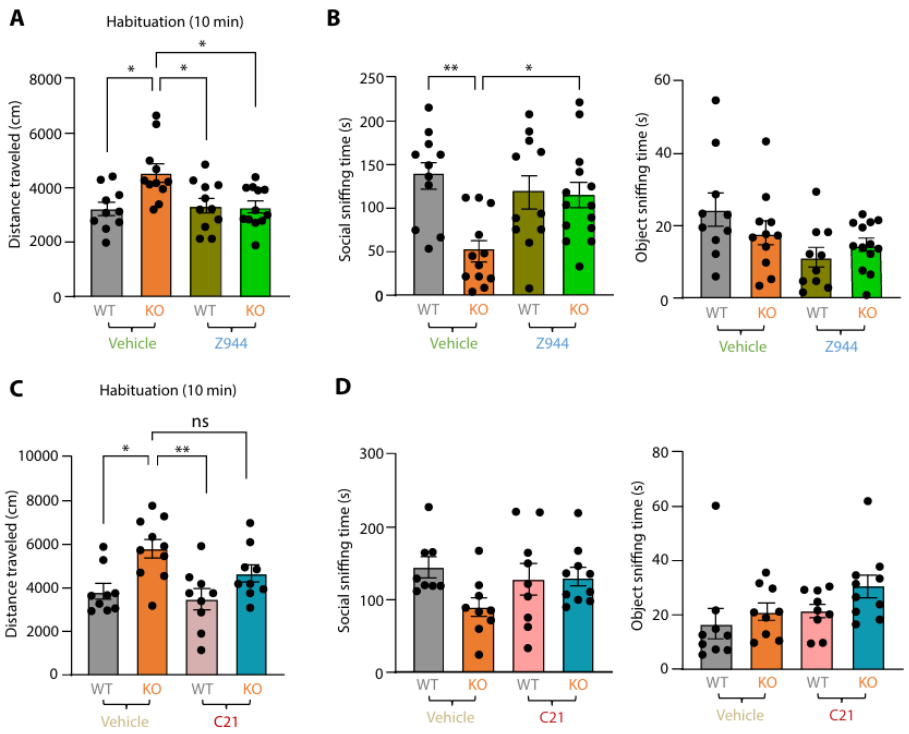

Fig. S7. Locomotor activity during habituation period and sniffing time (social and object) following either inhibition of T-type calcium channels or activation of hM4D(Gi) in RT neurons. **(A)** Quantification of total distance traveled during habituation period (10 min) with vehicle or Z944. (n = 10 for *Cntnap2*$^{+/+}$-Veh, n = 11 for *Cntnap2*$^{-/-}$-Veh, n = 11 for *Cntnap2*$^{+/+}$-Z944, n = 12 for *Cntnap2*$^{-/-}$-Z944). **(B)** Quantification of social (left) and object (right) sniffing time over 10 min with vehicle or Z944. (n = 11 for *Cntnap2*$^{+/+}$-Veh, n = 11 for *Cntnap2*$^{-/-}$-Veh, n = 10 for *Cntnap2*$^{+/+}$-Z944, n = 13 for *Cntnap2*$^{-/-}$-Z944). **(C)** Quantification of total distance traveled during habituation period (10 min) with vehicle or C21. (n = 9 for *Cntnap2*$^{+/+}$-Veh, n = 10 for *Cntnap2*$^{-/-}$-Veh, n = 9 for *Cntnap2*$^{+/+}$-C21, n = 9 for *Cntnap2*$^{-/-}$-C21). **(D)** Quantification of social (left) and object (right) sniffing time over 10 min with vehicle or C21. (n = 8 for *Cntnap2*$^{+/+}$-Veh, n = 9 for *Cntnap2*$^{-/-}$-Veh, n = 9 for *Cntnap2*$^{+/+}$-C21, n = 10 for *Cntnap2*$^{-/-}$-C21). The statistical tests involved two-way ANOVA with Tukey's test (A-B). Data are represented as mean values ± SEM. *P*-values in figure panels: **P* < 0.05; ***P* < 0.01.

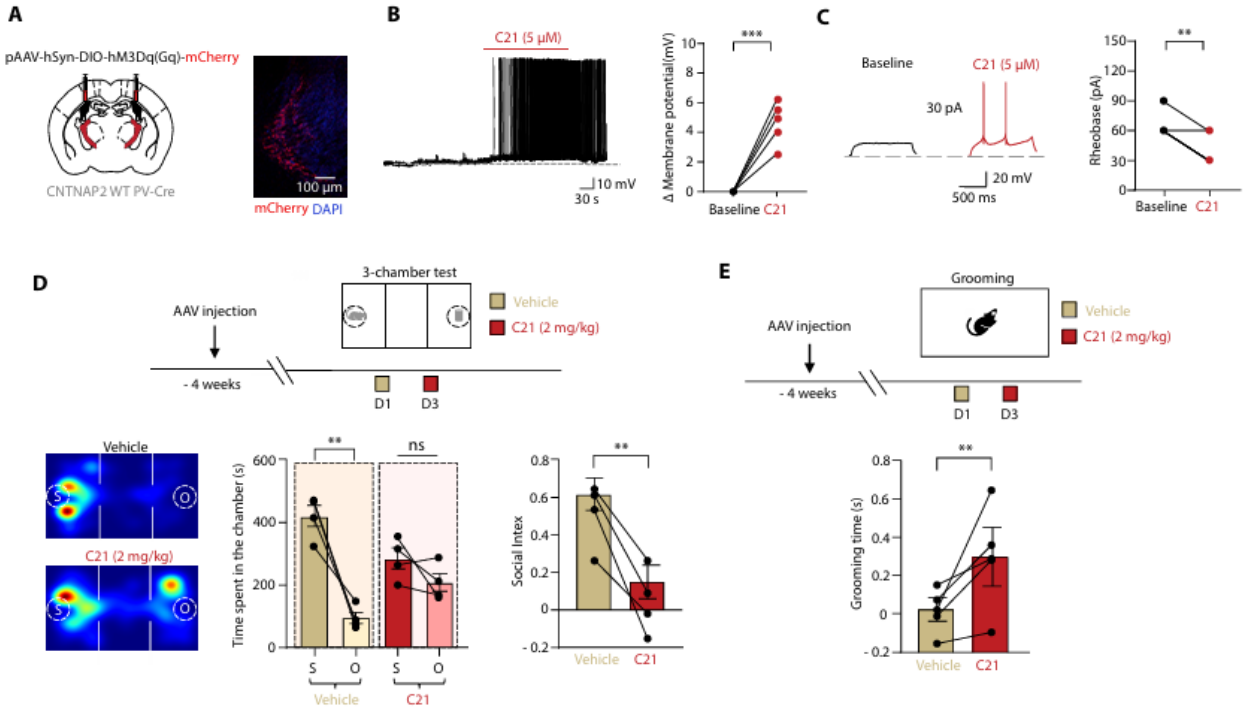

Fig. S8. Chemogenetic activation of RT impairs social preference and grooming behavior in *Cntnap2*$^{+/+}$ mice. (A) Schematic (left) describing stereotaxic injection of pAAV-hSyn-DIO-hM3D(Gq)-mCherry into RT and red fluorescence (right) representing expression of mCherry. **(B)** Representative trace (left) showing membrane potential after C21 and quantification (right) of C21-induced changes in membrane potential. (n = 5). **(C)** Representative traces (left) showing APs elicited by rheobase current and quantification (right) of C21-induced changes in rheobase current. (n = 6). **(D)** Experimental strategy (top) for evaluating the effect of chemogenetic RT activation on social preference, representative heatmaps (bottom, left) showing location during the social preference tests, and quantification of time spent in the chamber (bottom, middle) and the social index (bottom, right) in *Cntnap2*$^{+/+}$ PV-Cre expressing hM3Dq mice treated with vehicle or C21. **(E)** Experimental strategy (top) for evaluating the effect of chemogenetic RT activation on grooming behavior and quantification (bottom) of grooming time in *Cntnap2*$^{+/+}$ PV-Cre expressing hM3Dq mice treated with vehicle or C21. The statistical tests involved a paired two-tailed t-test (B-E). Data are represented as mean values ± SEM. *P*-values in figure panels: $^{**}P < 0.01$; $^{***}P < 0.001$.

Caption for Movie S1. Behavioral monitoring under light conditions with fiber photometry recording. Representative video showing a freely moving mouse under light conditions during simultaneous behavioral monitoring and fiber photometry recording. The optic fiber was implanted into RT region. This video was edited down to 20 secs from a total 10 min recording and is reflected in Fig. 5D.

Caption for Movie S2. Behavioral monitoring under dark conditions with fiber photometry recording. Representative video showing a freely moving mouse under dark conditions during simultaneous behavioral monitoring and fiber photometry recording. The optic fiber was implanted into RT region. This video was edited down to 20 secs from a total 10 min recording and is reflected in Fig. 5D.

Caption for Movie S3. Behavioral monitoring (baseline) before social interaction under light conditions with fiber photometry recording. Representative video showing a freely moving mouse under light conditions with simultaneous behavioral monitoring and fiber photometry recording before social interaction. The optic fiber was implanted into RT region. This video was edited down to 20 secs from a total 10 min recording and is reflected in Fig. 5E.

Caption for Movie S4. Behavioral monitoring during social interaction under light conditions with fiber photometry recording. Representative video showing a freely moving mouse under light conditions with simultaneous behavioral monitoring and fiber photometry recording during social interaction. The optic fiber was implanted into RT region. This video was edited down to 20 secs from a total 10 min recording and this 20-sec clip shown here corresponds to the time window from 4:22 to 4:42 after the start of the social interaction, during a period of active interaction with a novel conspecific. This video is reflected in Fig. 5E.

Caption for Movie S5. Behavioral monitoring in an empty cage under light conditions with fiber photometry recording. Representative video showing a freely moving mouse in an empty cage under light conditions with simultaneous behavioral monitoring and fiber photometry recording. The optic fiber was implanted into RT region. This video was edited down to 20 secs from a total 10 min recording and is reflected in Fig. 5F.

Caption for Movie S6. Behavioral monitoring in a cage filled with objects under light conditions with fiber photometry recording. Representative video showing a freely moving mouse in a cage filled with objects under light conditions with simultaneous behavioral monitoring and fiber photometry recording. The optic fiber was implanted into RT region. This video was edited down to 20 secs from a total 10 min recording and is reflected in Fig. 5F.

Caption for Movie S7. Behavioral monitoring (baseline) before PTZ injection under light conditions with fiber photometry recording. Representative video showing a freely moving mouse under light

conditions with simultaneous behavioral monitoring and fiber photometry recording. The optic fiber was implanted into RT region. This video was edited down to 20 secs from a total 10 min recording before PTZ injection and is reflected in Fig. 5G.

Caption for Movie S8. Behavioral monitoring after PTZ injection under light conditions with fiber photometry recording. Representative video showing a freely moving mouse under light conditions with simultaneous behavioral monitoring and fiber photometry recording. The optic fiber was implanted into RT region. This video was edited down to 20 secs from a total 10 min recording and this 20-sec clip shown here corresponds to the time window from 8:11 to 8:31 after PTZ injection and is reflected in Fig. 5G.